A Compartmental Model for Alveolar Clearance of Pertechnegas

Jörg Kotzerke, Jörg van den Hoff, Wolfgang Burchert, Thomas O.F. Wagner, Matthias Emter and Heinz Hundeshagen
Departments of Nuclear Medicine, Radiology and Pulmology, Center for Internal Medicine Medical School Hannover, Germany

The washout of an inhaled water soluble radiotracer from the lungs is a measure of alveolar integrity. Data evaluation of ^{99m}Tc-DTPA studies were previously performed mainly with monoexponential fitting with or without background subtraction. The introduction of ^{99m}Tc-pertechnegas for the assessment of alveolar permeability necessitates the investigation of adequate data evaluation schemes for this radiotracer. **Methods:** We developed a three-compartmental model to describe ^{99m}Tc-pertechnegas kinetics after inhalation. Monoexponential fitting of the first 5 min was investigated as simplification for clinical use. Different background corrections based on blood samples or representative regions of interest were compared. **Results:** Correction of intra- and extravascular background by subtraction of calibrated curves, which are derived from blood or background areas, resulted in monoexponential washout curves. Clearance rates based on the three-compartmental model were nearly the same as those derived from a monoexponential fit after blood-activity subtraction ($r = 0.96$). A monoexponential analysis of the first 5 min without any background correction correlates well with the first component of the biexponential analysis ($r = 0.97$). **Conclusion:** A dynamic study of more than 45 min allows quantitative determination of the transfer rate of ^{99m}Tc-pertechnegas from the alveoli into the blood using compartmental analysis. A simplified monoexponential analysis of the first 5 min allows assessment of lung clearance without any background correction.

Key Words: radionuclide; pertechnegas; alveolar permeability

J Nucl Med 1996; 37:2066–2071

Since the initial description of radionuclide aerosol lung imaging in 1965 by Taplin et al. (*1,2*), the aerosol technique has been used for ventilation-perfusion imaging and evaluation of alveolar capillary membrane integrity. After alveolar deposition, a water-soluble substance diffuses into the blood through the surfactant, basal membrane, interstitium and vessel endothelium. The speed of this diffusion is an indicator of the integrity of the alveolar capillary barrier (*3*). In smokers and in patients with fibrotic lungs, this integrity is disrupted, causing strongly increased washout (*4,5*). So far, [^{99m}Tc]DTPA has usually been used to measure alveolar integrity. Now, however, the technegas generator provides a more attractive alternative for producing dehydrated ^{99m}Tc-pertechnetate as a pseudo gas or ultrafine aerosol (*6*). Compared to [^{99m}Tc]DTPA, pertechnegas has the practical advantage of being an initially dry aerosol that reacts with the moisture in the airway. The size of the aerosol particles is about 0.17 μm, which leads to a minor bronchial deposition of only 5% (*7*). The amount of radioactivity deposited in the lungs can easily be regulated by the radioactivity simmered in the boat and is inhaled sufficiently with a single breath.

A decisive factor for the rate of elimination from the alveoli into the blood is particle size (*3*). Pertechnetate (mol wt: 163) has proven to have much faster kinetics than larger ^{99m}Tc-DTPA molecules (mol wt: 492). Quantitative assessment of tracer clearance from the lungs necessitates background correction from intra- and extravascular space, either by subtraction before data fitting or by including the background in the fitting procedure. One common correction method requires an additional tracer injection to calibrate the background curve (*8*). Alternatively, a representative area from the field-of-view of a gamma camera (i.e., shoulder, inter-renal area and liver) can be used for correction (*9*). The derived background curve is subtracted from the lung curve after possible scaling with an empirical adaption factor (*10*).

In this study, we investigated to what extent empirical background correction, by use of a reference region, can be justified within the context of an adequate compartmental model. For clinical applications, we investigated to what extent monoexponential data evaluation, without any background correction, can be utilized. We compared the standard approaches for background subtraction with a two-compartment model resulting from a simplification of a more detailed three-comparment model (see Appendix).

MATERIALS AND METHODS

We use a three-compartment model to describe the tracer kinetics after alveolar deposition of a ^{99m}Tc-pertechnetate aerosol (Fig. 1). The tracer is transported from the lung (compartment L) into the intravascular space (compartment I) with a rate k_1. The tracer is then exchanged with the extravascular space (compartment E) or eliminated from the detector field of view by excretion or trapping in certain organs.

Because the detector covers different fractions of the compartment volumes, the measured time-activity curve is given by the superimposition:

$$m(t) = f_L m_L(t) + f_I m_I(t) + f_E m_E(t), \qquad \text{Eq. 1}$$

where $m_x(t)$ is the amount of tracer in compartment x at time t and f_x is the fraction of compartment x covered by the detector. The solution of the differential equations describing the model is given in the Appendix. Our data evaluation is based on Equation A9 (see Appendix), which takes into account that the equilibration between intra- and extravascular space is much faster than the rate of excretion. Equation A9 yields a biexponential decrease of measured activity over the lung:

$$m(t) = f_L m_0 \cdot [(1 - B)e^{-k_1 \cdot t} + B \cdot e^{-k_a \cdot t}] \qquad \text{Eq. 2}$$

where

$$k_a = \frac{k_4}{k_3 + k_4} k_2 . \qquad \text{Eq. 3}$$

The amplitude B is determined by the rate constants and covered background fractions as given in the appendix. This equation allows the direct determination of the rate of tracer clearance from

Received Dec. 5, 1995; revision accepted Apr. 3, 1996.
For correspondence or reprints contact: Jörg Kotzerke, MD, Radiologie III (Nuklearmedizin), Universitätsklinikum, D-89070 Ulm, Germany.

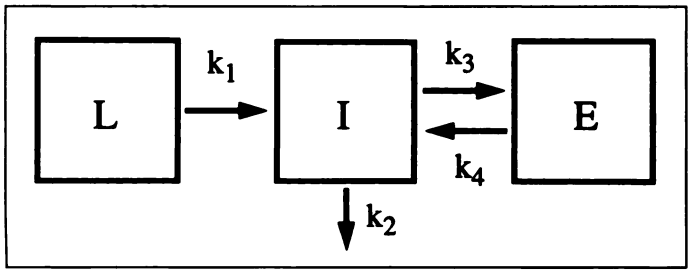

FIGURE 1. Kinetics of alveolar deposited pertechnegas or pertechnetate. Tracer is transported from the lungs (compartment L) into the intravascular space (compartment I) with a rate k_1. Tracer is then exchanged with the extravascular space (compartment E) or is eliminated from the field of view by excretion or trapping in certain organs.

the lung, k_1, as well as assessment of the effective rate of excretion from intra- and extravascular space, k_a.

Due to the slow excretion rate, quantitative determination of k_1 requires data acquisitions of 45–60 min. Because much shorter acquisitions are required in a clinical setting, we investigated how the parameter estimates are affected by evaluating the initial phase of the lung clearance curve with a simple monoexponential fit. In the limit $k_1 t \ll 1$, $k_a t \approx 0$ first order Taylor expansion of the exponentials ($e^{-kt} \approx 1 - kt$) in Equation A9 leads to:

$$m = f_L m_0[(1 - B)(1 - k_1 t) + B]$$

$$= f_L m_0(1 - (1 - B)k_1 t) = f_L m_0 e^{-(1-B)k_1 t}. \quad \text{Eq. 4}$$

The initial phase of lung clearance is approximately monoexponential. In this limit, the monoexponential fit yields a rate $k_m = (1 - B)\, k_1$ instead of the true lung clearance. It is remarkable that the relation between k_m and k_1 is strictly linear as long as B is a constant.

Aerosol Production and Application

Pertechnegas is produced by a technegas generator using a mixture of 97% argon and 3% oxygen (*6,11*). We simmered 500 MBq ^{99m}Tc in a 0.14-ml volume crucible. Patients inhaled the aerosol with a single deep breath in the supine position. Initially, deposited activity was found to be 60.000 ± 12.500 cpm over the right lung. This guaranteed sufficient statistical accuracy. Aquisition started directly after exhalation of the nondeposited activity.

Patients

Thirteen patients (7 women, 6 men; age range 45 ± 15 yr) were investigated; seven were smokers and one suffered from sarcoidosis (Table 1).

Aquisition

Dynamic studies of 45 min (6 patients; 90 frames) and 60 min (7 patients; 120 frames) were aquired from the posterior view using a large field of view gamma camera with a parallel-hole collimator. Fifteen minutes after inhalation, venous blood samples were taken at 2-min intervals and then every 5 min.

Data Analysis

To eliminate the influence of the blood pool in the heart region and excreted activity in the stomach, only the right lung was used for data evaluation. The lung region was determined with a 20% isocontour using the integral image of the first 3 min. For definition of the different background regions (shoulder, inter-renal and liver), care was taken to avoid activity in the thyroid, stomach and kidneys. Decay-corrected curves were transferred to a SUN-workstation (SUN Microsystems) for further analysis using Matlab (Mathworks Inc.). A Simplex algorithm was used for the nonlinear fitting.

RESULTS

Background Correction with Measured Blood Samples

After 45–60 min, the measured activity over the lung is essentially background activity. Therefore, the activity from the last blood samples was scaled to the activity over the lung. The corrected blood curve was finally subtracted from the washout curve (Fig. 2). This results in a good linearity during the first 20 min in a semilogarithmic plot (Fig. 3).

Background Correction with Various Regions of Interest

Background regions most frequently suggested in literature for measurements with a gamma camera are shoulder, inter-renal region and liver. These background curves were scaled in the same way as the blood samples using the late frames from the lung regions of interest (ROIs) and compared with the actual measured blood activity. Scaling factors obtained for the shoulder, inter-renal and liver were: 2.34 ± 0.39 (range: 1.66–2.86), 1.59 ± 0.30 (range: 1.08–2.29) and 1.45 ± 0.20 (range: 1.12–1.1.84), respectively. The differently corrected

TABLE 1
Clinical Data, Technical Details and Fitting Results

Patient no.	Age (yr)	Sex	Smoker (cigarettes per day)	Study length (min)	Initial right lung activity (cpm)	k_1 (1/min)	k_{cor} (1/min)	k_{mono} (1/min)
1	24	F		45	34390	0.104	0.109	0.078
2	33	M	10	45	34456	0.122	0.116	0.079
3	49	F		45	37708	0.089	0.108	0.064
4	45	F	Sarcoidosis	45	25212	0.118	0.103	0.083
5	67	M	20	45	45696	0.177	0.162	0.119
6	64	F		45	25726	0.073	0.092	0.052
7	71	M		60	32832	0.109	0.112	0.080
8	39	M		60	16912	0.070	0.068	0.051
9	36	F		60	56700	0.077	0.080	0.060
10	53	M	20	60	56128	0.130	0.131	0.102
11	37	M	20	60	23020	0.143	0.149	0.112
12	36	F	10	60	30110	0.084	0.093	0.061
13	40	F	15	60	48250	0.085	0.085	0.072
average					35934	0.106	0.108	0.078
s.d.					12533	0.031	0.027	0.022

Clearance rate constants: k_1 = compartmental analysis; k_{cor} = blood background subtraction; k_{mono} = monoexponential analysis of the first 5 min.

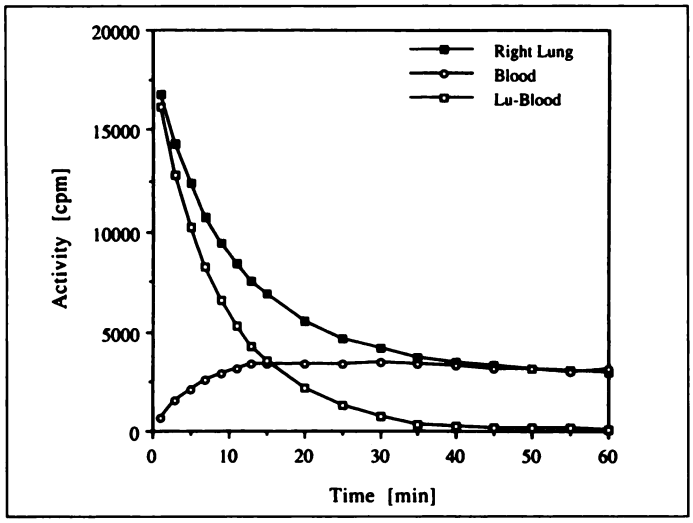

FIGURE 2. Example of background correction with calibrated blood-activity curve in a single patient. Calibration is obtained by normalization of the blood acitivity to the last 5 min of the lung clearance curve.

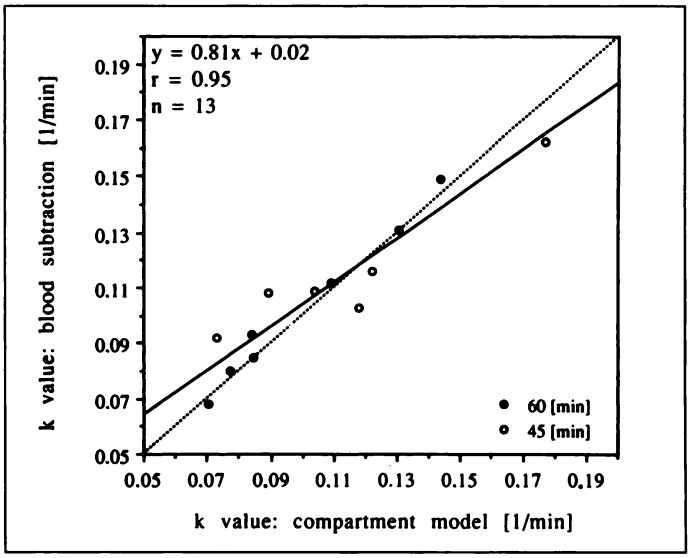

FIGURE 4. Clearance rates, k_{cor}, obtained with background correction using a scaled blood curve compared to clearance rates, k_1, derived from biexponential analysis of the data sets. Solid line represents best fit of a straight line. Line of identity is indicated by dotted line. Closed circles indicate 60-min studies.

lung washout curves became linear in a semilogarithmic plot (Fig. 3).

Use of a Three-Compartmental Model

The lung clearance, k_1, resulting from the biexponential fit according to Equation A9 was compared to the rate k_{cor} derived from monoexponential fitting of the data corrected for blood background in Figure 4. A good linear correlation between k_1 and k_{cor} is obvious, especially for the 60-min studies. The average difference (i.e., the mean value of the fractional deviations between the individual k_1, k_{cor} values) of both values was only about 3%. By using the compartmental analysis for all data, the amplitude B of the second exponential (reflecting essentially the relative background contribution to the lung ROI [see Appendix]) was determined as 19% ± 4% (range 11%-31%). Biexponential fitting only worked well for the sufficiently long acquisition times. The effect of shortening the acquisition time was assessed by comparing results from fitting the complete data with fitting of successively reduced data sets (Fig. 5). Shown are k_1 values of reduced data sets normalized to the k_1 values derived from fits to the complete time course. The fits became rapidly unstable for measurements shorter than 45 min.

Monoexponential Analysis

The correlation of a monoexponential analysis of the first 5 min of the curve and the fast component of the biexponential procedure is given in Figure 6. The linear correlation obtained is good, but the regression line deviates significantly from the line of identity, as expected from the theoretical considerations. Increasing the time interval for the monoexponential fit was investigated in Figure 7. At high clearance levels, the monoex-

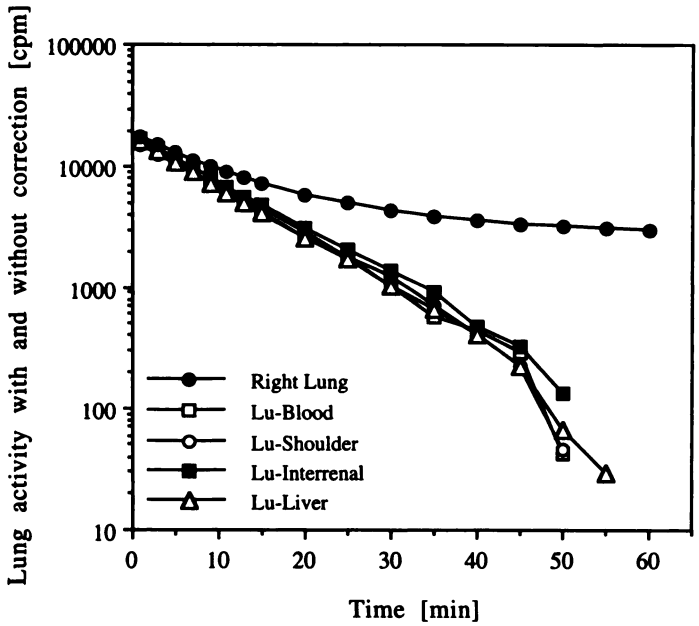

FIGURE 3. Lung activity after subtraction of normalized background curves in a single patient (semilogarithmic scale). Corrected curves are always monoexponential. Corrected curves have decreased to less than 1% of their initial values after 45 min and drop virtually to zero until 60 min.

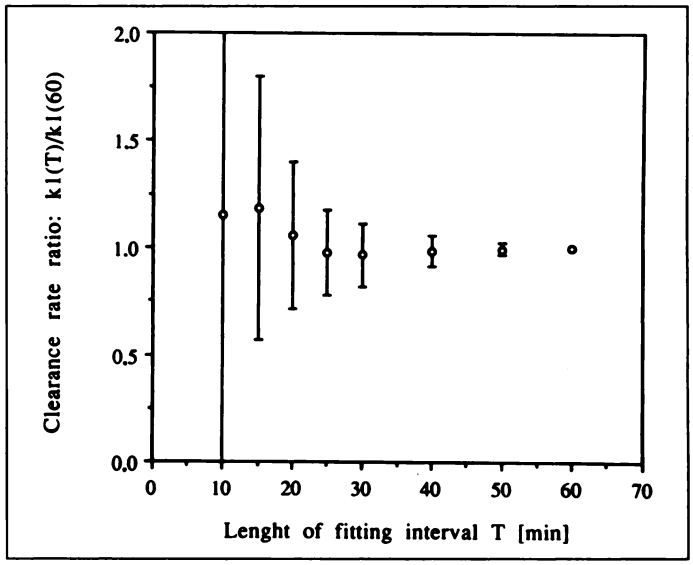

FIGURE 5. Influence of acquisition duration on statistical accuracy of k_1. Results are averages of overall patients. k_1 (T) values normalized to the values derived from fits to the complete time course are shown. Error bars indicate average difference between results from restricted and complete fitting intervals. Errors increase rapidly for acquisition times shorter than about 40 min.

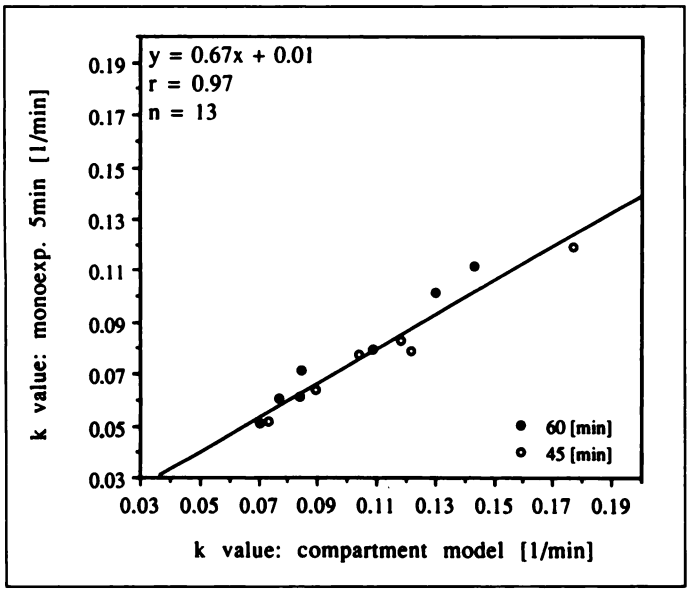

FIGURE 6. Correlation of the k values derived from monoexponential analysis of the first 5 min, k_{mono}, and biexponential analysis ot the complete data sets, k_1. Solid line represents best fit of a straight line. Closed circles indicate 60-min studies.

ponential rates deviate drastically from the true clearance levels if the fitting interval was extended much beyond 5 min.

DISCUSSION

Although measurements of alveolar permeability using tracer techniques have been established for over 15 yr (*12*), there are still methodological problems that have not been solved. One problem is related to radiotracer application. When using a jet nebulizer and [^{99m}Tc]DTPA, an inhalation period of 3 min or more is usually necessary for a deposition of 10 MBq activity (*3,13*). During this period, inhalation, diffusion and excretion are superimposed. A second problem concerns particle size and deposition pattern in the lungs. Depending on the nebulizer, the [^{99m}Tc]DTPA aerosol has a particle size of about 0.5–3 μm, resulting in a sizable bronchial deposition, which must be considered (*14–17*). Compared to [^{99m}Tc]DTPA, pertechnegas has the practical advantage to be an initially dry aerosol, which reacts with the moisture in the airway. The size of the aerosol particles is about 0.17 μm which leads to a minor bronchial deposition of only 5% (*7*). The amount of radioactivity deposited in the lungs can easily be regulated by the radioactivity simmered in the boot and is inhaled sufficiently with a single breath. In contrast to [^{99m}Tc]DTPA, the short clearance times also allow clearance rate decreases to occur.

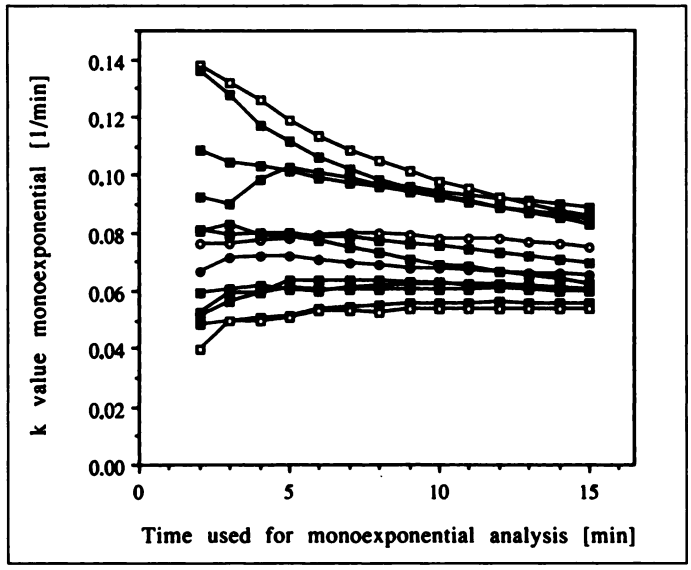

FIGURE 7. Dependence of monoexponential clearance rates on fitting interval duration for all 13 patients. Strong dependence at high clearance rates is obvious. Nevertheless, a good linear relationship between k_{mono} and k_1 is maintained for short fitting interval durations (Fig. 6).

The activity counting technique is another problem. Initially, probes were used to measure lung and background activity over the patients limbs (*8*). Background correction was done using a second tracer application and calculating a correction factor for the background curve (*3*). A correction with multiple blood samples and different tracers was proposed by Groth et al. (*18*), which is not feasible for clinical use. Published correction factors for the subtraction of various background areas range from 0.87 for an inter-renal area to 1.94 for a ROI over the shoulder (*10*). However, Peters et al. (*19*) demonstrated that the liver is the most suitable reference organ for background correction. Since both corrections (using blood activity from multiple samples and adapted background curves) results in a linear decrease of lung activity in semilogarithmic representation (Fig. 3), the basic assumption of a simple diffusion process of ^{99m}Tc-pertechnegas from the alveolar space into the blood seems justified. Additionally, the large variation of the scaling factor in different patients indicates that a subtraction based on mean values may probably lead to large errors.

To date, compartmental models to measure alveolar permeability have only been suggested for [^{99m}Tc]DTPA. Peterson et al. (*20*) assumed up to three different compartments for their animal studies to investigate the influence of lung volume on permeability. Köhn et al. (*14*) used a compartment model to calculate the transfer rate by means of the excreted activity in the urine. The model presented here suggests biexponential analysis of the lung washout curve, where the fast component corresponds to the transfer into the blood and the slow component represents a mixture of intra- and extravascular activity and their clearance. Within the context of our model, k_2 is the rate of irreversible loss of the tracer from the ROI over the right lung. Therefore, it accounts for excretion as well as irreversible trapping in various organs. According to our data, this process occurs at a rate of about 25% per hour. It seems reasonable to treat this process as slow in comparison to the rate of back-transport from the extravascular space. Adopting this interpretation separation of intra- and extravascular activity is impossible because of rapid equilibration of both pools and the comparable sizes of the covered volume fractions (Eqs. A7, A8). This reduces the three-compartment model essentially to a two-compartment model with only one effective background compartment. It is cleared with an effective rate k_a (Eq. A5), which is smaller than the clearance rate k_2 from the intravascular space. It should be stressed that only the interpretation of the slow exponential is affected by this question and not the determination of the lung clearance rate.

Our results show that the biexponential approach requires data acquisitions of at least 45 min for a reliable determination of the fitting parameters. It is obvious from Figure 4 that especially clearance values derived from 60 min studies are close to the line of identity. Therefore, it is possible to determine quantitatively the lung clearance rate k_1. The results (k_1: 0.106 ± 0.032/min) agree within 3% with those obtained after individually scaled background correction and monoexponential fitting over 20 min (k_{cor}: 0.108 ± 0.027/min). However, like the biexponential approach, individual background scaling requires acquisition of at least 45 min.

On the other hand, it is possible to describe the early phase of the clearance curve by a monoexponential decrease whose decay constant, k_m, is reduced by a certain factor in comparison to the lung clearance. This is generally correct for biexponential curves. In the present case, the reduction factor (1-B) is defined by the compartment model (Eq. A9). Because k_a is much smaller than k_1, the amplitude B is virtually independent of k_1. B is essentially determined by the size of the covered background fraction and does vary interindividually over a certain range (0.11–0.31 in our data). Therefore, the reduction factor (1-B) varies accordingly (0.69–0.89 in our data), but the variation is fractionally small (only about ± 10% with respect to the average). Thus, the model predicts that the clearance rate as derived from a monoexponential fit of the first few minutes yields an approximately constant underestimation of the true clearance rate. The underestimation according to our data is expected to be about 0.8 if the fitting interval is extremely short. In practice, we have chosen a fitting interval of 5 min as a compromise in order to achieve sufficient statistical accuracy.

Figure 6 shows that the predicted linear relationship between k_1 and k_m can be observed. This proves that the actual interindividual variations of the parameter B are quantitatively unimportant as far as the linear relation between k_1 and k_m is concerned. The reduction factor is somewhat smaller than the expected value, namely 0.67. Using only the more reliable 60 min data, a slope of 0.78 is obtained. A slight reduction of the slope relative to the expected value of 0.8 is a consequence of choosing a fitting interval of 5 min which does not strictly satisfy the assumption $k_1 t \ll 1$. Nevertheless, the linear relation between k_1 and k_m is maintained for our fitting interval. Extending the monoexponential fitting over substantially larger fitting intervals does lead to deviations from this linear relation at elevated clearance rates. This is obvious from Figure 7 which shows that the ratios of different k_m vary drastically at elevated clearance rates if fitting is extended beyond 5 min.

Because of the observed good linear correlation between k_1 and k_m, a simple 5-min acquisition and a monoexponential fit without any background subtraction seems best suited for application in a clinical environment (*21*). This finding justifies the empirical approach of Rinderknecht et al. (*12*) who assessed lung clearance with ^{99m}Tc-DTPA and ^{99m}Tc-pertechnetate and estimated clearance rates from monoexponential fits of the first 7 min without background corrections. In contrast to approaches based on background subtraction with average scaling and fitting intervals of 15 min or more, the derived k_m values are not sensitive to individual deviations from the average background contribution. In principle, the true lung clearance, k_1, can be calculated quantitatively from the measured k_m by use of the regression line determined in Figure 6. It should be stressed, however, that the important information is already given by the k_m themselves. All follow-up investigations or interindividually comparisons can be performed with these monoexponential rates because of their constant relationship to the true lung clearance.

CONCLUSION

We have compared three strategies for the evaluation of lung clearance rates: (a) empirical background subtraction followed by monoexponential fitting over 15 min or more, (b) biexponential fitting based on a three-compartment model and (c) monoexponential fitting over 5 min without any background correction. The first approach yields only accurate results if the background subtraction is optimized individually which necessitates long acquisitions of at least 45 min. Average scaling of the background curves can lead to uncontrollable errors. The second approach allows quantitative determination of the lung clearance without independent background determination but requires long acquisitions of at least 45 min. Finally, the third approach yields clearance rates that are strongly linearly correlated to lung clearance over the physiological range. We propose the latter approach as being best suited for application in a clinical setting.

APPENDIX

The model equations corresponding to Figure 1 are:

$$\frac{dm_L}{dt} = -k_1 m_L ,$$

$$\frac{dm_I}{dt} = k_1 m_L - (k_2 + k_3) m_I + k_4 m_E ,$$

$$\frac{dm_E}{dt} = -k_3 m_I - k_4 m_E . \qquad \text{Eq. A1}$$

The solution of Equation A1 for a bolus inhalation at time zero is (⊗: convolution, m_0: total dose deposited in lungs):

$$m_L(t) = m_0 \cdot e^{-k_1 \cdot t} ,$$

$$m_I(t) = m_L(t) \otimes \frac{k_1}{\lambda_b - \lambda_a} [(k_4 - \lambda_a) \cdot e^{-\lambda_a \cdot t} - (k_4 - \lambda_b) \cdot e^{-\lambda_b \cdot t}] ,$$

$$m_E(t) = m_L(t) \otimes \frac{k_1 k_3}{\lambda_b - \lambda_a} [e^{-\lambda_a \cdot t} - e^{-\lambda_b \cdot t}] , \qquad \text{Eq. A2}$$

with the decay constants

$$\lambda_{a/b} = \frac{k_2 + k_3 + k_4}{2} - / + \sqrt{\left(\frac{k_2 + k_3 + k_4}{2}\right)^2 - k_2 k_4} . \qquad \text{Eq. A3}$$

The measured time-activity curve is given by the superposition

$$m = f_L m_L + f_I m_I + f_E m_E , \qquad \text{Eq. A4}$$

where fx is the fraction of compartment x covered by the detector. Empirically, a sum of two exponentials is sufficient to fit the patient data; the residues between data and fit show no systematic trend which would indicate the presence of a third exponential. Introducing a third exponential leads only to instabilities during the fit and large uncertainties of the parameter estimates. On the other hand, Equations A2 and A4 yield in general a sum of three exponentials (corresponding to the number of compartments in the model). The number of exponentials is reduced by assuming rapid exchange between intra- and extravascular space in comparison to the slow excretion. In this limit ($k_2 \ll k_4$) Equation A3 can be rewritten (using first-order Taylor expansion):

$$\lambda_a \approx k_a = \frac{k_4}{k_3 + k_4} k_2 ,$$

$$\lambda_b \approx k_b = k_3 + k_4 , \qquad \text{Eq. A5}$$

and m_I, m_E are approximated by:

$$m_I \approx m_L(t) \otimes \frac{k_1}{k_3 + k_4} (k_4 \cdot e^{-k_a \cdot t} + k_3 \cdot e^{-k_b \cdot t}),$$

$$m_E \approx m_L(t) \otimes \frac{k_1}{k_3 + k_4} (k_3 \cdot e^{-k_a \cdot t} - k_3 \cdot e^{-k_b \cdot t}). \qquad \text{Eq. A6}$$

The background contribution is thus given by:

$$m_B = m_L(t) \otimes \frac{k_1}{k_3 + k_4} [(f_I k_4 + f_E k_3) \cdot e^{-k_a \cdot t} + (f_I - f_E) \cdot e^{-k_b \cdot t}]. \qquad \text{Eq. A7}$$

The second exponential in Equation A7 can be neglected for two reasons: the covered fractions of intra-and extravascular space are similar ($f_I \approx f_E$) and the exponential decays rapidly because exchange between intra- and extravascular space is assumed to be fast ($k_b \gg k_a$). Therefore, Equation A7 reduces to:

$$m_B = m_L(t) \otimes \frac{k_1}{k_3 + k_4}(f_I k_4 + f_E k_3) \cdot e^{-k_a \cdot t}. \quad \text{Eq. A8}$$

By combining Equations A1, A4 and A8 one finally obtains:

$$m = f_L m_L + m_B, = f_L m_0[(1 - B) \cdot e^{-k_1 \cdot t} + B \cdot e^{-k_a \cdot t}],$$

where

$$B = \frac{k_1}{k_1 - k_a}\left(\frac{f_I k_4 + f_E k_3}{f_L(k_3 + k_4)}\right). \quad \text{Eq. A9}$$

Therefore, the time-activity curve has a biexponential shape and the decay constants of the exponentials are the lung clearance, k_1, and the elimination rate out of the background, k_a. Further identifiable parameters are the observed fraction of the total deposited dose, $f_L m_0$ and the amplitude of the second exponential, B.

If $f_I \approx f_E$ or $k_3 \approx k_4$, B can be rewritten as:

$$B = \frac{k_1}{k_1 - k_a} \cdot \frac{f_B}{f_L} \quad \text{Eq. A10}$$

where

$$f_B = \frac{f_I + f_E}{2} \quad \text{Eq. A11}$$

is the average background fraction from intra- and extravascular space. In this case B does not depend on k_3, k_4, and the fit yields the relative background f_B/f_L.

REFERENCES

1. Taplin GV, Poe ND. A dual lung scanning technique for evaluation of pulmonary function. *Radiology* 1965;85:365–368.
2. Taplin GV, Poe ND, Greenberg A. Lung scanning following radioaerosol inhalation. *J Nucl Med* 1966;7:77–87.
3. Jones JC, Minty BD, Royston D. The physiology of the leaky lungs. *Br J Anaesth* 1982;54:705–721.
4. Effros RM, Mason GR. Measurements of pulmonary epithelial permeability in vivo. *Am Rev Respir Dis* 1983;127:S59–S65.
5. Huchon GJ, Russel JA, Barritault LG, Lipavsky A, Murray JF. Chronic airflow obstruction does not increase epithelial permeability assessed by aerosolized solute but smoking does. *Am Rev Respir Dis* 1984;130:457–460.
6. Monaghan P, Provan I, Murray C, et al. An improved radionuclide technique for the detection of altered pulmonary permeability. *J Nucl Med* 1991;32:1945–1949.
7. Lloyd JJ, Shields RA, Taylor CJ, Lawson RS, James JM, Testra HJ. Technegas and pertechnegas particle size distribution. *Eur J Nucl Med* 1995;22:473–476.
8. Barrowcliffe MP, Otto C, Jones JG. Pulmonary clearance of [^{99m}Tc]DTPA: influence of background activity. *J Appl Physiol* 1988;64:1045–1049.
9. O'Doherty MH, Page CJ, Croft DN, Bateman NT. Lung [^{99m}Tc]DTPA transfer: a method for background correction. *Nucl Med Commun* 1985;6:209–215.
10. Langford JA, Lewis CA, Gellert AR, Tolfree SEJ, Rudd RM. Pulmonary epithelial permeability: vascular background effects on whole lung and regional half-time values. *Nucl Med Commun* 1986;7:183–190.
11. Scalzetti EM, Gagne GM. The transition from technegas to pertechnegas. *J Nucl Med* 1995;36:267–269.
12. Rinderknecht J, Shapiro L, Krauthammer M, et al. Accelerated clearance of small solutes from the lungs in interstitial lung disease. *Am Rev Respir Dis* 1980;121:105–117.
13. Groth S, Hermansen F, Rossing N. Pulmonary permeability in never smokers between 21–67 yr. *J Appl Physiol* 1989;67:422–428.
14. Köhn H, König B, Klech H, Pohl W, Mostbeck A. Urine excretion of inhaled technetium-99m-DTPA: an alternative method to assess lung epithelial transport. *J Nucl Med* 1990;31:441–449.
15. Bennett WD, Ilowite JS. Dual pathway clearance of [^{99m}Tc]DTPA from bronchial mucosa. *Am Rev Respir Dis* 1989;139:1132–1138.
16. Groth S, Hermansen F, Rossing N. Pulmonary clearance of inhaled [^{99m}Tc]DTPA: significance of site of aerosol deposition. *Clin Physiol* 1990;10:85–98.
17. Oberdörster G, Utell MJ, Morrow PE, Hyde RW, Weber DA. Bronchial and alveolar absorption of inhaled [^{99m}Tc]DTPA. *Am Rev Respir Dis* 1986;134:944–950.
18. Groth S, Lassen NA, Rossing N. Determination of the mean transit time for the transport of aerosolized ^{99m}Tc-DTPA across the pulmonary eptihelial membrane. A plasma sample method. *Clin Physiol* 1988;8:93–103.
19. Peters AM, Mason GR, Hughes JMB. Appropriate background subtraction for pulmonary radioaerosol clearance [Abstract]. *J Nucl Med* 1992;33:836.
20. Peterson BT, James HL, McLarty JW. Effects of lung volume on clearance of solutes from the air spaces of lungs. *J Appl Physiol* 1988;64:1068–1075.
21. Kotzerke J, Strumpf A, Emter M, Hundeshagen H. Kinetische Analyse und Normwerte für die Messung der alveolaren Permeabilität mit Pertechnegas (PTG) [Abstract]. *Nuklearmedizin* 1994;33:A46.